Original Article

Effects of heavy ions ($^{12}C^{6+}$) on malignant melanoma B16F10 cells

Li-Ping Zhang[1,2], Sha Li[2], Hong Zhang[3], Qiang Li[3], Yang Liu[3], Fei-Fei Li[1], Da-Jie Gong[1]

[1]Department of Life Science, Northwest Normal University, Lanzhou, China; [2]Department of Radiation Oncology, the 940th Hospital of Joint Logistics Support Force of Chinese People's Liberation Army, Lanzhou, China; [3]Department of Radiation Medicine, Institute of Modern Physics, Chinese Academy of Sciences, Lanzhou, China

Contributions: (I) Conception and design: LP Zhang, S Li; (II) Administrative support: DJ Gong; (III) Provision of study materials or patients: H Zhang, Q Li; (IV) Collection and assembly of data: Y Liu, FF Li; (V) Data analysis and interpretation: Y Liu, FF Li; (VI) Manuscript writing: All authors; (VII) Final approval of manuscript: All authors.

Correspondence to: Da-Jie Gong, PhD. Department of Life Science, Northwest Normal University, No. 967 of Anning East Road, Anning District, Lanzhou 730070, China. Email: gongdajie88_dr@163.com; Sha Li, MM. Department of Radiation Oncology, The 940th Hospital of Joint Logistics Support Force of Chinese People's Liberation Army, No. 333 of Nanbinhe Road, Chengguan District, Lanzhou 730050, China. Email: lisha2233_dr@163.com.

Background: This study aimed to investigate the effects of heavy ion ($^{12}C^{6+}$) irradiation on the proliferation, apoptosis, cell cycle, migration, and epithelial-mesenchymal transition (EMT) of B16F10 cells.

Methods: The B16F10 cells, which is a malignant melanoma cell line widely used in research, irradiated by $^{12}C^{6+}$ and X-ray were detected by Hoechst 33342/propidium iodide double staining, Western blot, flow cytometry, and cell scratch tests to evaluate cell proliferation, expression of apoptosis-related proteins, G2/M phase arrest, cell migration, cell invasion and EMT.

Results: Compared with the same physical X-ray dose, $^{12}C^{6+}$ could effectively inhibit the proliferation of B16F10 cells, inhibit the expression of B-cell lymphoma-2 (Bcl-2) and cellular-myelocytomatosis viral oncogene (c-Myc), and induce the expression of Bax to promote the apoptosis of B16F10 cells. After $^{12}C^{6+}$ irradiation, the B16F10 cells exhibited G2/M phase arrest. B16F10 cells were highly sensitive to $^{12}C^{6+}$ irradiation. Moreover, compared with X-ray, the $^{12}C^{6+}$ irradiation significantly inhibited the migration of B16F10 cells and inhibited extracellular matrix cleavage, induced E-cadherin expression, enhanced cell adhesion, and further inhibited cell invasion, migration, and EMT.

Conclusions: The B16F10 cells were highly radiosensitive to $^{12}C^{6+}$. Compared with X-ray, B16F10 cells irradiated by $^{12}C^{6+}$ significantly reduced the expressions of matrix metalloproteinases to inhibit extracellular matrix cleavage and, thus, effectively inhibit cell invasion and metastasis. However, although the issue of the different therapeutic effects of heavy ion and X-ray radiotherapy on malignant melanoma was investigated and preliminary research results were obtained, several problems must be further studied.

Keywords: Malignant mouse melanoma B16F10 cell; heavy ion ($^{12}C^{6+}$); X-ray; radiosensitivity; invasion; metastasis

Submitted Aug 20, 2021. Accepted for publication Mar 17, 2022.
doi: 10.21037/tcr-21-1692
View this article at: https://dx.doi.org/10.21037/tcr-21-1692

Introduction

Malignant melanoma is a type of malignant skin tumor with strong invasiveness and migration, high incidence and high mortality. It usually occurs on the surface of skin and the mucous membrane of organs (1). The primary clinical treatment methods for this disease are surgery, chemotherapy, immunotherapy, and radiotherapy (2). The related chemotherapy treatment mainly consists of the use of a combination of drugs, mainly including dacarbazine (DTIC); the objective response rate of treatment is 7–13%. In some treatments, DTIC is replaced by the chemotherapeutic drugs temozolomide and fotemustine; however, they aren't shown to have better effects than DTIC. At present, immunotherapy has the best clinical effect; the objective response rate of programmed cell death

protein 1 (PD-1) monoclonal antibody inhibitor is 40.0%, but its clinical use is limited (3-5). Therefore, radiotherapy is considered a standard form of clinical treatment for malignant melanoma. However, a previous clinical trial revealed that malignant melanoma is not sensitive to conventional radiotherapy (X-ray, γ-ray, and electron-ray) (6). Under this treatment, the disease easily recurs and has a high distal metastasis rate; patients usually die of lung metastasis (6). After $^{12}C^{6+}$ radiotherapy, patients' local control rates are significantly improved (7-9), suggesting that this is an important method in the treatment of malignant melanoma. After DNA is damaged by irradiation, ataxia telangiectasia mutated (ATM) and related proteins in cells can conduct injury signals and cause cell cycle regulation, making the cell cycle arrest at two checkpoints: the G1/S and G2/M phases; then, G1 phase arrest and G2 phase arrest occur (10-15). The sensitivity of cells to irradiation decreases in this order: M phase, G2 phase, G1 phase, early S phase, and late S phase. Cells are the most sensitive in the M phase and least sensitive in the S phase (16). Therefore, G2/M checkpoint arrest is an important determinant of the radiosensitivity of tumor cells. Malignant melanoma has strong invasiveness and mobility; hence, it has a high recurrence rate and distal migration rate during clinical treatment. The mortality rate of such patients is higher than that of other skin cancer patients (17). The invasion and metastasis of a malignant tumor is a complex physiological process. After epithelial-mesenchymal transition (EMT), the intercellular adhesion ability is decreased, leading to stronger cell mobility, promoting the invasion and metastasis of malignant tumor cells at the levels of morphological development and transcription (18). E-cadherin is a marker of EMT. A decrease in E-cadherin expression can lead to a decrease in cell adhesion and an increase in cell migration (19-21). Moreover, matrix metallopeptidase (MMP)-2 and MMP-9 are also involved in tumor migration and invasion, affecting the metastasis ability of tumors. In the early invasion process of a tumor, transforming growth factor-β (TGF-β) induces an increase in MMP-2 and MMP-9 expression and promotes the degradation of the basement membrane to reduce or even eliminate the contact inhibition of tumor cells, allowing them to obtain stronger mobility and invasiveness (22,23). In addition, a previous study also reported that by inhibiting MMP-2 and MMP-9 through the Phosphatidylinositide 3-kinases/protein kinase B (PI3K/Akt) signaling pathway, luteolin can inhibit the proliferation and induce apoptosis of human malignant melanoma cells *in vivo* and *in vitro* (24).

This study aimed to investigate the effects of heavy ion ($^{12}C^{6+}$) irradiation on the proliferation, apoptosis, cell cycle, migration, and EMT of B16F10 cells. The B16F10 cells irradiated by $^{12}C^{6+}$ and X-ray were detected by Hoechst 33342/propidium iodide (PI) double staining, Western blot, flow cytometry, and cell scratch tests to evaluate cell proliferation, expression of apoptosis related proteins, G2/M phase arrest, cell migration, cell invasion and EMT. We present the following article in accordance with the MDAR reporting checklist (available at https://tcr.amegroups.com/article/view/10.21037/tcr-21-1692/rc).

Methods

Reagents and instruments

Dulbecco's Modified Eagle's Medium (DMEM, Hyclone, Illinois, USA), trypsin (Hyclone, USA), phosphate-buffered saline (PBS, Hyclone, USA), fetal bovine serum (FBS, BI, Israel, USA), dimethyl sulfoxide (Sigma, St. Louis, Missouri, USA), a Cell Counting Kit-8 (CCK-8 Kit) (Dojindo, Kumamoto, Japan), cell cycle staining buffer (Multi Sciences, Hangzhou, China), Hoechst 33342/PI double staining kit (Solarbio, Beijing, China), antibodies (Abcam, Massachusetts, USA), petri dishes and culture flasks (Corning, New York, USA), and conventional reagents of analytical pure grade (Sinopharm, Shanghai, China).

Cell lines

The B16F10 cell line used was a mouse skin malignant melanoma cell line purchased from Shanghai Heyuan Biotechnology Co., Ltd. The cells were cultured in high-glucose DMEM with 10% FBS in a constant temperature incubator at 37 ℃ with 5% CO_2.

Irradiation conditions

The heavy ions ($^{12}C^{6+}$) were provided by the Heavy Ion Research Facility in Lanzhou (HIRFL), Institute of Modern Physics (IMP), Chinese Academy of Sciences, and the X-ray was provided by the 21EX medical linear accelerator of the 940 Hospital of the Joint Service Support Force of the Chinese People's Liberation Army. The B16F10 malignant melanoma cells were cultured in a 35- or 60-mm culture dish; while receiving X-ray irradiation, the irradiated cells were placed horizontally in the irradiated area.

The study was conducted in accordance with the

Declaration of Helsinki (as revised in 2013). The study was approved by ethics board of the 940th Hospital of Joint Logistics Support Force of Chinese People's Liberation Army (No. 2021KYLL233) and individual consent for this retrospective analysis was waived.

Hoechst 33342/PI double staining

When the cells grew approximately 60%, they were irradiated, placed into an incubator with 5% CO_2 at 37 ℃ for 48 h, and washed with PBS. Add 0.5-mL trypsin digestion solution to the overgrown cells and gently shake the dish to immerse the digestion solution into all the cell surfaces. After incubation in an incubator at 37 ℃ for about 1 min, the culture dishes were placed under an inverted microscope for observation. After cytoplasm retraction and stromal enlargement of the cells were found, digestion was immediately stopped with the medium containing serum. A cell staining solution was prepared according to a set ratio, and 1 mL of this solution was added to each dish of cells. The staining was conducted at 4 ℃ for 20–30 min. Then, the staining solution was discarded, and the cells were gently washed with PBS 2–3 times. Under a fluorescence microscope, ultraviolet light was used to excite the staining, and the observation and count were performed. In each group, a field of vision was randomly selected, from which the number of apoptotic cells and total number of cells (no less than 1,000 in each group) were calculated and the apoptotic rate was determined.

The procedures of irradiations

The absolute dose detection system used to calibrate the online dose-monitoring ionization chamber is sent annually to professional measurement and testing institutions such as the National Institute of Metrology of China (Changping District, Beijing) for compulsory calibration. Our measurement system followed the TRS398 report. The temperature and air pressure were calibrated before the dosage meter, and the electronic balance cap was used in ionization room. Moreover, the whole set was pre-started to warm up in advance, and the zeroing operation was balanced to reduce the system error after thermal balance.

Irradiations were performed with a carbon ion beam of 80.55 MeV/u in the heavy ion therapy terminal of the HIRFL at the IMP, Chinese Academy of Sciences. Dose averaged linear energy transfer (LET) value of the carbon ion beams on cell samples was adjusted to be 50 keV/μm according to our experimental requirements. X-rays irradiation was performed with an X-rays machine (RX-650, Tucson, AZ, USA) operating at 50 kVp. The dose rate was 0.4 Gy/min. In order to make sure the accuracy of the dose delivery, the real-time dose rate determinations were conducted under the similar radiation conditions with petri dishes. Then, the irradiated samples were evenly placed in the corresponding area of the sample plate. The irradiation position was 100 cm from the vacuum window and the field size was 5 cm. Range shift absorbers were 50-mm thick; scatters and broadening filters were not used. The built material was not covered during irradiation. We have made the independent dose verification in the place of the specimen using film during carbon ion irradiation, and one of the images is shown in Figure S1. What's more, before dose distribution, the absolute dose will be calibrated on the online dose monitoring ionization chamber. Meanwhile, the correspondence between the scale monitoring reading and the absolute dose will also ensure the accuracy of the irradiation dose. The irradiation position was 100 cm from the vacuum window and the field size was 5 cm. Meanwhile, energy absorbers with thickness of 50 mm were also added to ensure the accuracy of the irradiation energy delivered to the sample.

Detection of cell proliferation with the Cell Counting Kit-8 (CCK-8) Kit

The irradiated cells were digested, collected, and counted. Cell suspension was added to a 96-well plate with 2,000 cells/well. Each group had six duplicated wells, and wells with cell-free complete culture medium added were set as the negative control group. At 48 h after inoculation, 10 μL of CCK-8 was added to each well and cultured in the incubator for 2 h. The absorbance value at 450 nm was detected by an enzyme microplate reader. The absorbance value of each sample group was defined as the result of subtracting the absorbance value of a zeroing well from the average value of the absorbance value of a duplicated well. The cell survival rate was calculated according to the instructions. The method for calculating the relative biological effectiveness (RBE) comes from the paper of Yan *et al.* (24).

Detection of apoptosis with immunofluorescence

The cultured cells were irradiated. After 24 h, the cells were digested, collected in a 15-mL centrifuge tube,

and centrifuged at 1,000 rpm for three minutes at room temperature. Following this, the medium was discarded to collect the cell precipitate. Then, 300 μL of precooled 75% ethanol (prepared from PBS) was added, and the cells were re-suspended, fixed, and preserved at 4 ℃ overnight. After the cells were centrifuged at 1,500 rpm at room temperature, the ethanol solution was removed, PBS was added, and the cells were left standing for 15 min to rehydrate. The cells were washed via centrifugation three times, and the supernatant was discarded. Next, the cells were collected, and 1 mL of DNA staining solution and 10 μL of PI staining solution were added and shaken to mix. The cells were incubated in the dark at room temperature for 30 min and, finally, detected on a flow cytometer. According to the color difference of normal cells, apoptotic cells or necrotic cells after staining, the cells were observed and counted by ultraviolet light excitation under fluorescence microscope. Field was randomly selected in each group, the number of apoptotic cells and the total number of cells (no less than 1,000 in each group) were calculated, and the apoptotic rate was calculated.

Cell scratch test

The scratch assay was used to measure cell migration. The irradiated cells were washed with PBS, digested, and transferred to a 60-mm culture dish, with the cells just covering the dish after overnight inoculation as a suitable condition. A 200-μL sterile pipette tip was used to scratch vertically; the interval between lines was 1 cm. Then, PBS was used to gently wash the dish 2–3 times to remove any cells floating due to the scratches. After creating a "scratch" in a cell monolayer, a basic medium was added, and photos were immediately taken. The time point was set as 0 h, and the cells were cultured in an incubator with 5% CO_2 at 37 ℃. Photos were taken again after 48 h of culture. The cell migration rate was analyzed and calculated by the Image-Pro Plus software. Cell migration rate = (0-h scratch width – 48-h scratch width)/0-h scratch width ×100%.

Western blotting

Protein was extracted from the irradiated whole cells and quantified using bicinchoninic acid (BCA); then, the protein concentration was calculated and 20 microgram protein was loaded per lane. Sodium dodecyl sulfate polyacrylamide gel electrophoresis was performed until the protein marker was completely separated. Then, transmembrane was performed for 90 min with constant voltage of 100 V, and the protein was blocked using 5% skimmed milk powder for 2 h; a primary antibody was added, and the membrane was incubated overnight. Then, the membrane was washed with tris-buffered saline and Tween 20 (TBST), a secondary antibody was added, and the membrane was incubated. Following this, the membrane was washed with TBST again, luminescent liquid was added for exposure, and the gray values of the target bands were analyzed by Image-Pro Plus. Protein relative expression = gray value of target protein/gray value of β-actin. WB antibody was diluted with TBST at a ratio of 1:5,000 or 1:10,000. The proteins were collected 48 h post irradiation and then the expressions of proteins were detected by independent trials of Western blot analysis repeated for three times.

Flow cytometry analysis

Flow cytometric measurements were conducted to assess the cell cycle. Cells were harvested after the indicated treatment, fixed in 70% ice cold ethanol for 48 h, and stained in 0.2% Tritone X-100, 100 μg/mL RNase A and 50 μg/mL PI in PBS for 20 min. After filtered with 300 mesh nylon screen, the distributions of cell cycle phases were measured by flow cytometry (Becton Dickinson FACS Calibur, New York, USA).

Statistical methods

The experimental data were analyzed by the Image-Pro Plus and SPSS 23.0 software, and the Origin 9.0 software was used for drawing. The measurement data were expressed as the mean ± standard deviation and compared between two groups using a one-way analysis of variance (ANOVA). A value of $P<0.05$ was considered statistically significant.

Results

$^{12}C^{6+}$ irradiation causes morphological apoptosis changes in B16F10 cells

The *in-vitro*-cultured malignant mouse melanoma B16F10 cells were long fusiform-adherent cells with a clear boundary. After $^{12}C^{6+}$ irradiation, the growth and morphology of the cells were observed under an inverted phase contrast microscope. Adherent cells presented irregular morphology, nuclear pyknosis, slow proliferation, an unclear edge boundary, and mostly present mitosis,

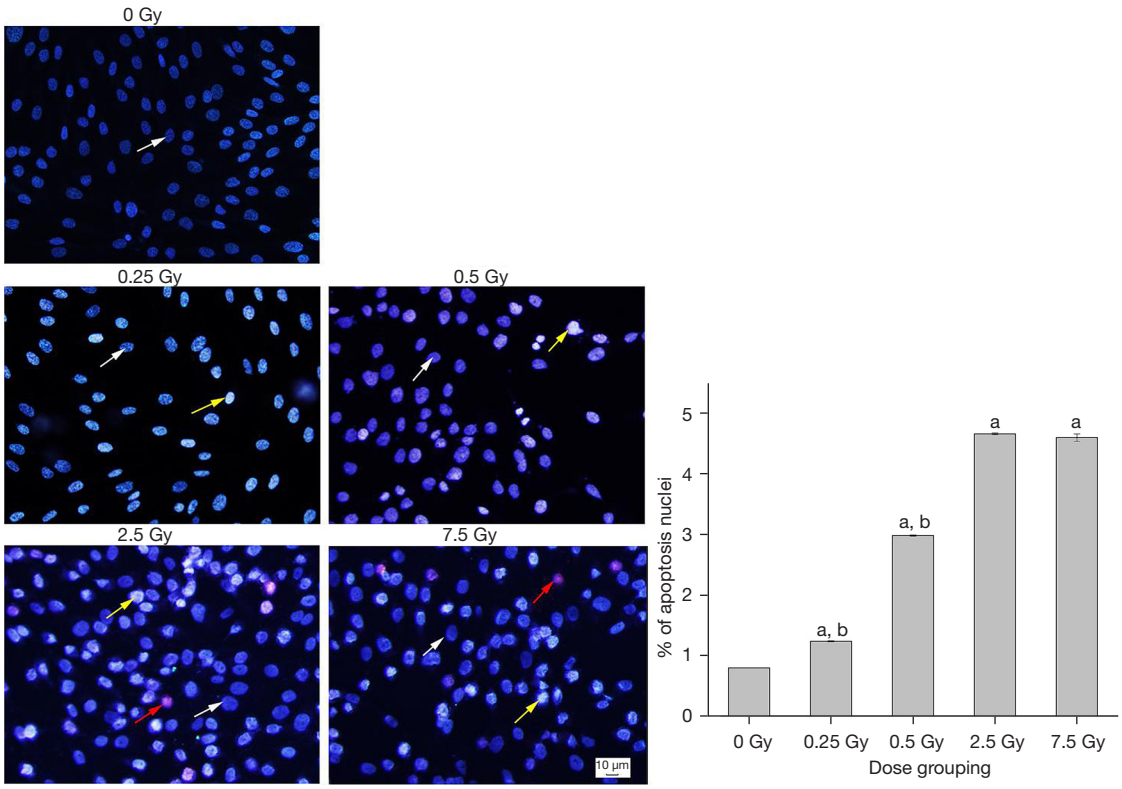

Figure 1 Morphological observation results and statistical data of B16F10 cell apoptosis induced by heavy ion ($^{12}C^{6+}$) irradiation. Hoechst 33342/propidium iodide double staining. The white arrow indicates normal cells, the yellow arrow indicates early apoptotic cells, the red arrow indicates late apoptotic or necrotic cells. [a], the comparison between the $^{12}C^{6+}$ irradiation group and the blank control group (P<0.05); [b], the intra-group comparison within the $^{12}C^{6+}$ irradiation group (P<0.05).

showing a gradual trend of dissolution; the number of necrotic cells was gradually increased. The apoptosis morphology of the cells was detected via Hoechst 33342/PI double staining, after which the cells were photographed with a fluorescent microscope. The results are shown in *Figure 1*.

Referring to the relative biological effect, it shows that the relative biological effects of carbon ions are higher than the X-ray from 2.5 to 3 Gy, according to the clonogenic survival assay (25). The control group (0 GyE) was B16F10 cells without $^{12}C^{6+}$ irradiation. Meanwhile, B16F10 cells irradiated with 0.25 and 0.5 GyE of $^{12}C^{6+}$ irradiation were bright blue after staining, or the nucleus was lobulated, fragmentary, and concentrated in the cell border; these cells were in the early stage of apoptosis. Regarding B16F10 cells irradiated with 2.5 and 7.5 GyE $^{12}C^{6+}$ irradiation, in addition to the presence of early apoptotic cells, there were several malignant mouse melanoma B16F10 cells with reddish or crimson nuclei; these cells were all late apoptotic or necrotic cells. After the intra-group comparison between the $^{12}C^{6+}$ irradiation groups, the results revealed that the apoptotic cells occurred primarily after 2.5 GyE of irradiation (P<0.05), indicating that $^{12}C^{6+}$ irradiation can induce apoptosis of B16F10 cells (*Figure 1*).

$^{12}C^{6+}$ irradiation inhibits proliferation of B16F10 cells

The B16F10 cells were cultured *in vitro* and irradiated by 0.25, 0.5, 2.5, and 7.5 GyE of $^{12}C^{6+}$. The CCK-8 method was used to detect the 450-nm absorbance of the cells irradiated with different doses of $^{12}C^{6+}$. The detection results are shown in *Figure 2A*. As shown in the figure, the absorbance values of the B16F10 cells irradiated by all doses of $^{12}C^{6+}$ were lower than that of the control group (0 GyE), and the differences were statistically significant (P<0.05). Moreover, the results revealed that the absorbance decreased gradually as the irradiation dose increased; the absorbance value was lowest at the 2.5-GyE dose, but when the dose increased to 7.5 GyE, the absorbance value did not decrease significantly compared with the

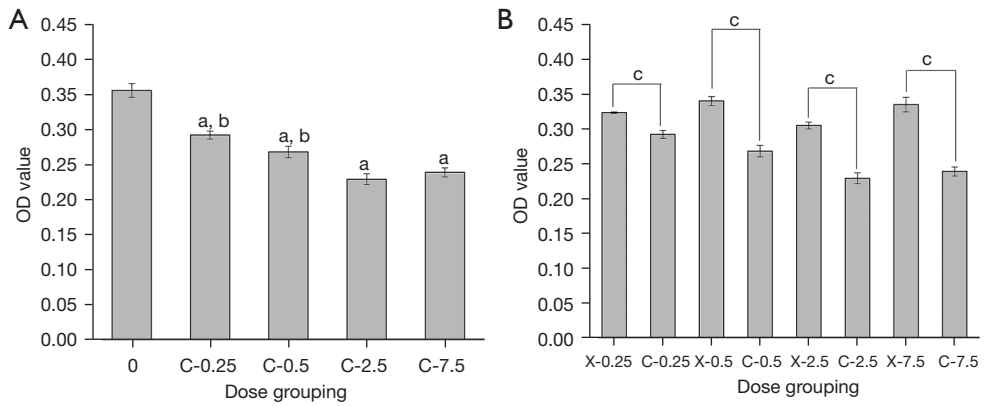

Figure 2 Effects of $^{12}C^{6+}$ and X-ray irradiation on the proliferation of B16F10 cells. (A) The comparison between the $^{12}C^{6+}$ irradiation group and the blank control group (^{a}, P<0.05). ^{b}, the intra-group comparison of $^{12}C^{6+}$ irradiation group, P<0.05; (B) the comparison between the $^{12}C^{6+}$ irradiation group and the X-ray irradiation group of the same dose (^{c}, P<0.05). C-0.25, C-0.5, C-2.5, C-7.5 represent $^{12}C^{6+}$ irradiation group at 0.25, 0.5, 2.5 and 7.5 Gy, respectively; X-0.25, X-0.5, X-2.5, X-7.5 represent X-ray irradiation group at 0.25, 0.5, 2.5 and 7.5 Gy, respectively. OD, optical density.

former dose (P>0.05). Thus, the $^{12}C^{6+}$ irradiation significantly inhibited proliferation of the B16F10 cells, and the inhibition effect was the most significant at the dose of 2.5 Gy.

To further understand the effects of $^{12}C^{6+}$ and conventional rays (e.g., X-ray) on the proliferation of B16F10 cells, the B16F10 cells were cultured *in vitro* and irradiated with 0.25, 0.5, 2.5, and 7.5 GyE of $^{12}C^{6+}$ and X-ray. Again, CCK-8 was used to detect the 450-nm absorbance of the cells irradiated with different doses. The detection results are shown in *Figure 2B*. As shown in the figure, the absorbance value of the B16F10 cells irradiated by all $^{12}C^{6+}$ doses was lower than that of the cells irradiated by all X-ray doses (P<0.05). The results also revealed that compared with X-ray, the $^{12}C^{6+}$ irradiation could significantly inhibit the proliferation of the B16F10 cells.

$^{12}C^{6+}$ irradiation causes changes in the expression of apoptosis-related proteins in B16F10 cells

The B16F10 cells were cultured *in vitro* and irradiated with 0.25, 0.5, 2.5, and 7.5 GyE of $^{12}C^{6+}$ and X-ray. Then, the protein was extracted, and the protein concentration was detected with a BCA quantitative kit. The protein loading was calculated, and Western blotting was used to detect the expressions of Bax, Bcl-2, and c-Myc in the B16F10 cells. The detection results are shown in *Figure 3*. As shown in the figure, compared with the control group (0 GyE), the expression of Bcl-2 was decreased, while the expressions of Bax and c-Myc were significantly increased in the cells irradiated by $^{12}C^{6+}$ (P<0.05). The expressions also increased as the irradiation dose increased, but when the irradiation dose was 7.5 GyE, there was no significant difference in the protein expressions compared with those at 2.5 GyE (P>0.05). The results also revealed that after $^{12}C^{6+}$ irradiation, the B16F10 cells underwent apoptosis, which was most significant at the dose of 2.5 GyE. Moreover, after the $^{12}C^{6+}$ irradiation, the expression of Bcl-2 was significantly lower than that after X-ray irradiation, and the expressions of Bax and c-Myc were significantly higher than those after X-ray irradiation. Thus, compared with X-ray, $^{12}C^{6+}$ could significantly induce the expression of apoptosis proteins in the B16F10 cells and inhibit the expression of anti-apoptotic proteins to induce apoptosis.

$^{12}C^{6+}$ irradiation induces G2/M phase arrest of B16F10 cells

The radiosensitivity of cells is related to the distribution of the cell cycle phases. The sensitivity of cells in different cell cycle phases is also different. To investigate the effects of $^{12}C^{6+}$ irradiation on the distribution of the cell cycle phases of B16F10 cells, B16F10 cells were cultured *in vitro* and irradiated with 0.25, 0.5, 2.5, and 7.5 GyE of $^{12}C^{6+}$. Then, they were stained with fluorescent PI dye, and the changes in the distribution of their cell cycle phases was detected using flow cytometry. The detection results are shown in *Figure 4*. As shown in the figure, compared with the control group (0 GyE), after the B16F10 cells were irradiated by $^{12}C^{6+}$, there was no change in the proportion of cells in the G1 phase. However, the proportion of cells in the G2 phase

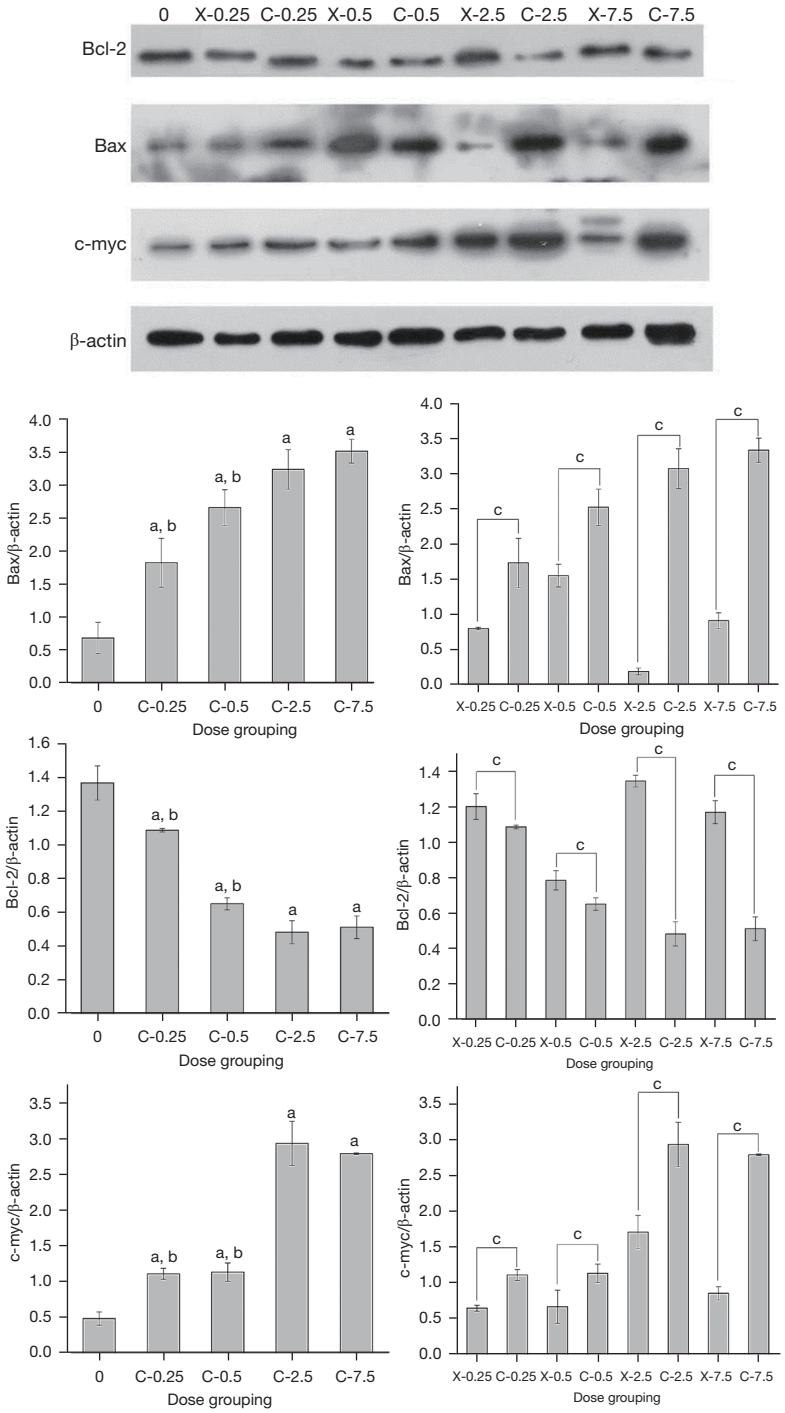

Figure 3 Effects of $^{12}C^{6+}$ and X-ray irradiation on the proliferation and apoptosis proteins of B16F10 cells and statistical data. The protein bands represent the protein expression levels of Bax, Bcl-2 and c-myc after different doses of $^{12}C^{6+}$ and X-ray irradiation. The histogram shows the relative protein expression level and statistical analysis obtained by systematically analyzing the gray value of the protein bands through Image-Pro Plus software. [a], the comparison between $^{12}C^{6+}$ irradiation group and blank control group, $P<0.05$; [b], the intra-group comparison of $^{12}C^{6+}$ irradiation group, $P<0.05$; [c], the comparison between the same dose of $^{12}C^{6+}$ and X-rays, $P<0.05$. C-0.25, C-0.5, C-2.5, C-7.5 represent $^{12}C^{6+}$ irradiation group at 0.25, 0.5, 2.5 and 7.5 Gy, respectively; X-0.25, X-0.5, X-2.5, X-7.5 represent X-ray irradiation group at 0.25, 0.5, 2.5 and 7.5 Gy, respectively.

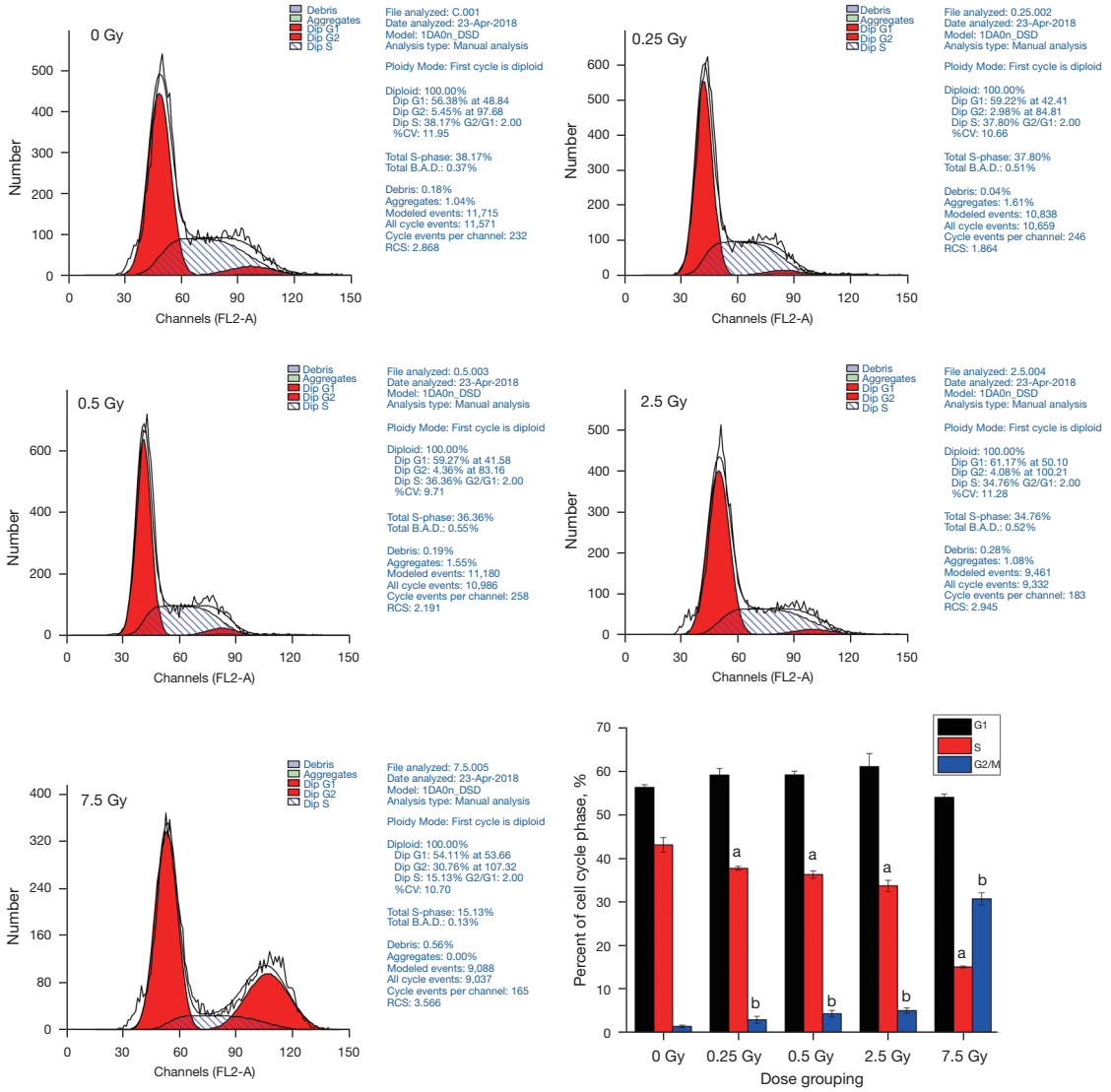

Figure 4 Effects of different doses of $^{12}C^{6+}$ irradiation on the distribution of cell cycle phases of B16F10 cells and statistical data. [a], the comparison of S-phase cells between the $^{12}C^{6+}$ irradiation group and the control group, $P<0.05$; [b], the comparison of G2/M phase cells in the $^{12}C^{6+}$ irradiation group and the control group, $P<0.05$.

gradually increased as the irradiation dose increased, and the proportion of cells in the S phase gradually decreased as the irradiation dose increased. The proliferation results revealed that after radiation, the proliferation of the cells was inhibited, while the cell cycle results revealed that the proportion of cells in the G2/M phase increased. Therefore, the results suggested that G2/M phase arrest occurred in the B16F10 cells after irradiation by $^{12}C^{6+}$. Cells in the G2/M phase are the most sensitive, further suggesting that the radiosensitivity of the B16F10 cells to the irradiation of $^{12}C^{6+}$ increased as the dose increased.

$^{12}C^{6+}$ irradiation decreases the migration rate of B16F10 cells

Malignant melanoma has a strong invasiveness and mobility, and its recurrence and distal migration rates are very high during clinical treatment, resulting in a very high patient mortality rate. To detect the effects of $^{12}C^{6+}$ and X-ray irradiation on the migration of B16F10 cells, the growth and migration of B16F10 cells at 48 h after irradiation were detected by a cell scratch test, and the cell migration rate was calculated and analyzed statistically. The detection results are shown in *Figure 5*. Compared

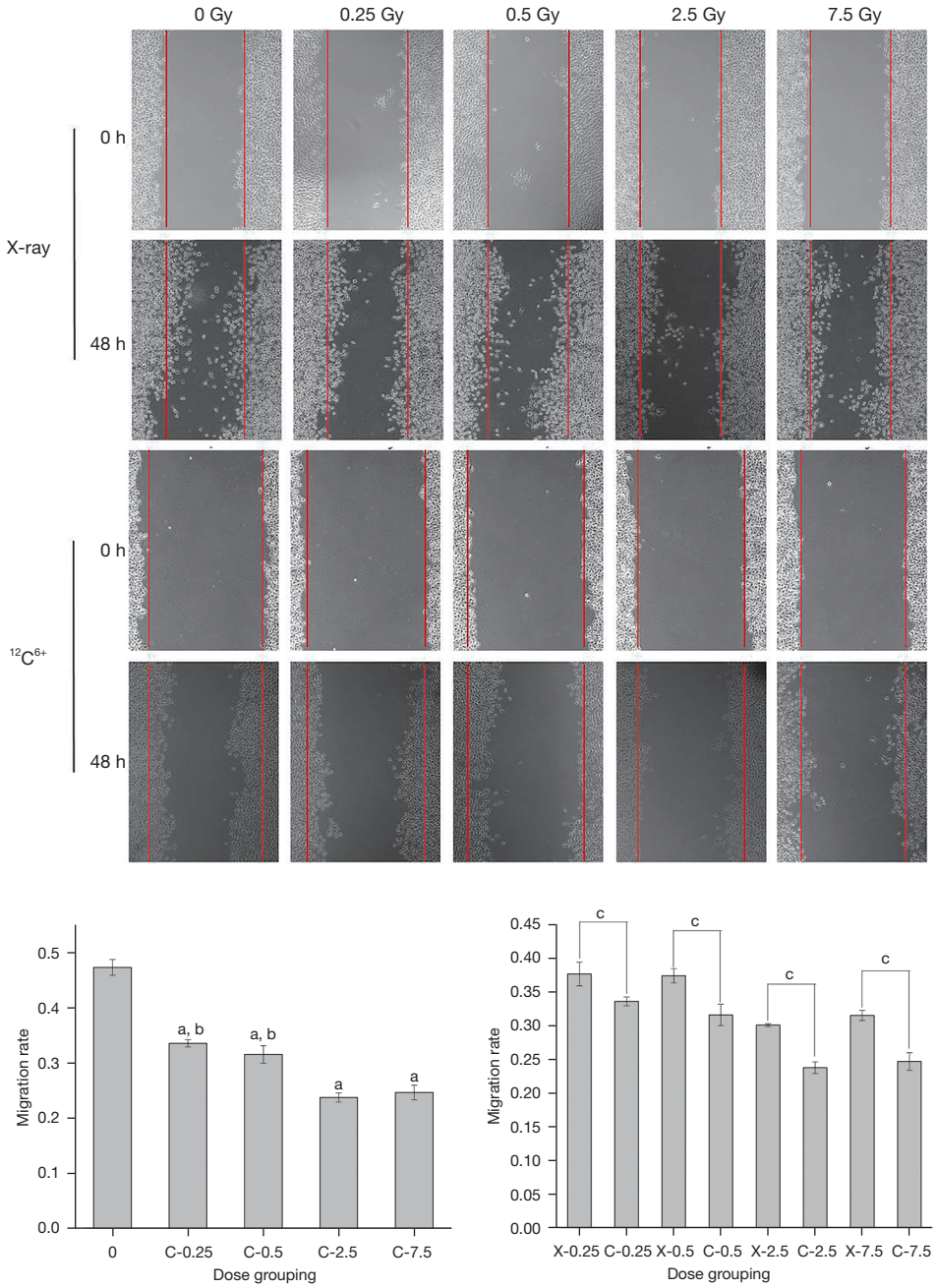

Figure 5 Effects of $^{12}C^{6+}$ and X-ray irradiation on the migration of B16F10 cells and statistical data. [a], the comparison between $^{12}C^{6+}$ irradiation group and blank control group, P<0.05; [b], the intra-group comparison of $^{12}C^{6+}$ irradiation group, P<0.05; [c], the comparison between the same dose of $^{12}C^{6+}$ and X-rays, P<0.05. C-0.25, C-0.5, C-2.5, C-7.5 represent $^{12}C^{6+}$ irradiation group at 0.25, 0.5, 2.5 and 7.5 Gy, respectively; X-0.25, X-0.5, X-2.5, X-7.5 represent X-ray irradiation group at 0.25, 0.5, 2.5 and 7.5 Gy, respectively.

with the control group (0 GyE), after $^{12}C^{6+}$ irradiation, the migration rate of the cells gradually decreased as the irradiation dose increased (P<0.05). The migration rate was lowest under the dose of 2.5 GyE of $^{12}C^{6+}$, but when the irradiation dose increased to 7.5 GyE, the migration rate was not significantly lower than that at 2.5 GyE (P>0.05). Compared with X-ray, the migration rate of cells inhibited by $^{12}C^{6+}$ was lower (P<0.05), indicating that $^{12}C^{6+}$ irradiation

can significantly inhibit the migration of B16F10 cells.

$^{12}C^{6+}$ irradiation inhibits the EMT of B16F10 cells

To detect the effects of $^{12}C^{6+}$ and X-ray irradiation on the EMT of B16F10 cells, Western blotting was used to detect the expressions of invasion-, migration-, and EMT-related proteins MMP-2, MMP-9, and E-cadherin. The detection results are shown in *Figure 6*. Compared with the control group (0 GyE), the expressions of MMP-2 and MMP-9 significantly increased after irradiation with 0.25 GyE of $^{12}C^{6+}$ ($P<0.05$) and significantly decreased after irradiation with 0.5, 2.5, and 7.5 GyE of $^{12}C^{6+}$ ($P<0.05$). The expression of E-cadherin decreased after irradiation with 0.25 and 0.5 GyE of $^{12}C^{6+}$ and significantly increased after irradiation with 2.5 and 7.5 GyE of $^{12}C^{6+}$; however, the differences were not statistically significant ($P>0.05$). The results revealed that irradiation with low doses of $^{12}C^{6+}$ could induce the expressions of MMP-2 and MMP-9 in B16F10 cells as well as inhibit the expression of E-cadherin. It may have also promoted EMT of the cells, and when the irradiation dose increased to 2.5 GyE, $^{12}C^{6+}$ inhibited the expressions of MMP-2 and MMP-9 and induced the expression of E-cadherin, thus significantly inhibiting the migration of the B16F10 cells. It can also inhibit EMT of B16F10 cells.

Discussion

Malignant melanoma is a highly malignant, radiation-resistant, and aggressive tumor insensitive to conventional radiotherapies. Heavy ion $^{12}C^{6+}$ can break the DNA double-strand in malignant melanoma cells, causing irreversible damage, so the effect of such radiotherapy is significant (10). In the present study, the proliferation of B16F10 cells irradiated by X-ray and $^{12}C^{6+}$ was detected via the CCK-8 method, revealing that the proliferation of B16F10 cells was significantly inhibited by $^{12}C^{6+}$ irradiation. The inhibition effect was the most significant at irradiation with 2.5 GyE of $^{12}C^{6+}$. Brenner *et al.* revealed that (10) heavy ion irradiation irreparably damages the DNA of B16F10 cells and inhibits their proliferation. In addition, the growth of B16F10 cells was observed by Hoechst 33342/PI double staining, and the results revealed that heavy ion irradiation can induce apoptosis of B16F10 cells. In the present study, the expressions of Bax, Bcl-2, and c-Myc were detected by Western blotting. The *Bcl-2* gene is the primary target molecule of research on the apoptosis molecular mechanism, which inhibits apoptosis (11). The expression of c-Myc is closely related to cell proliferation and apoptosis, and dysfunction of the *c-Myc* gene expression is the primary cause of apoptosis. The rate of apoptosis and its sensitivity to inducing factors depend on the content of the c-Myc protein. In immature thymocytes, high expression of the *c-Myc* gene is the cause of death of embryonic thymocytes, and high expression of this gene is also observed in the death stage of apoptotic cells (12). The present results revealed that compared with X-ray, after $^{12}C^{6+}$ irradiation, the expressions of Bax and c-Myc were significantly higher, while the expression of Bcl-2 was lower, suggesting that $^{12}C^{6+}$ can induce the expressions of apoptosis proteins in B16F10 cells to promote apoptosis.

In the present study, the distribution of the cell cycle phases of the B16F10 cells irradiated by $^{12}C^{6+}$ was detected by flow cytometry. The results revealed that the proportion of cells in the G2/M phase increased after irradiation, indicating that the $^{12}C^{6+}$ irradiation prolonged the G2/M phase arrest of the cells. This may be the primary cause of the high radiosensitivity of B16F10 cells to $^{12}C^{6+}$. In consistent with our findings, Aninditha found that a G2/M arrest was detected after photons or heavy ions (C^{12} and O^{16} ions) irradiation in a dose-dependent manner (26). Similarly, Saito and his colleagues also discovered that carbon ion irradiation induced G2/M cell cycle arrest (27).

In sum, the cancer-killing effects of $^{12}C^{6+}$ on malignant mouse melanoma B16F10 cells are strong. It can inhibit cell proliferation, reduce the expressions of anti-apoptotic proteins, induce the expressions of apoptosis proteins, and promote apoptosis. Moreover, $^{12}C^{6+}$ irradiation regulates the cell cycle and causes G2/M phase arrest. The results suggest that B16F10 cells have a high radiosensitivity to $^{12}C^{6+}$.

EMT-related proteins: epithelial cadherin, neurotype cadherin, vimentin, keratin, etc. The MMP family—MMP-2 and MMP-9 mainly hydrolyze the main type IV collagen of the basement membrane, disrupting the tissue barrier and allowing the tumor cells to undergo invasion and metastasis. In addition, MMP-2 also hydrolytically activates TGF-beta to promote epithelial-mesenchymal transition (EMT). MMP-9 promotes tumor angiogenesis through the release of vascular endothelial growth factor (VEGF). In the present study, the effects of X-ray and $^{12}C^{6+}$ irradiation on the invasion and migration of B16F10 cells were demonstrated by detecting the expressions of EMT-associated proteins MMP-2, MMP-9, and E-cadherin. The molecular markers of EMT, i.e., the expressions of MMP-2 and MMP-9, were decreased after both the X-ray and $^{12}C^{6+}$ irradiation. However, compared with X-ray, after $^{12}C^{6+}$

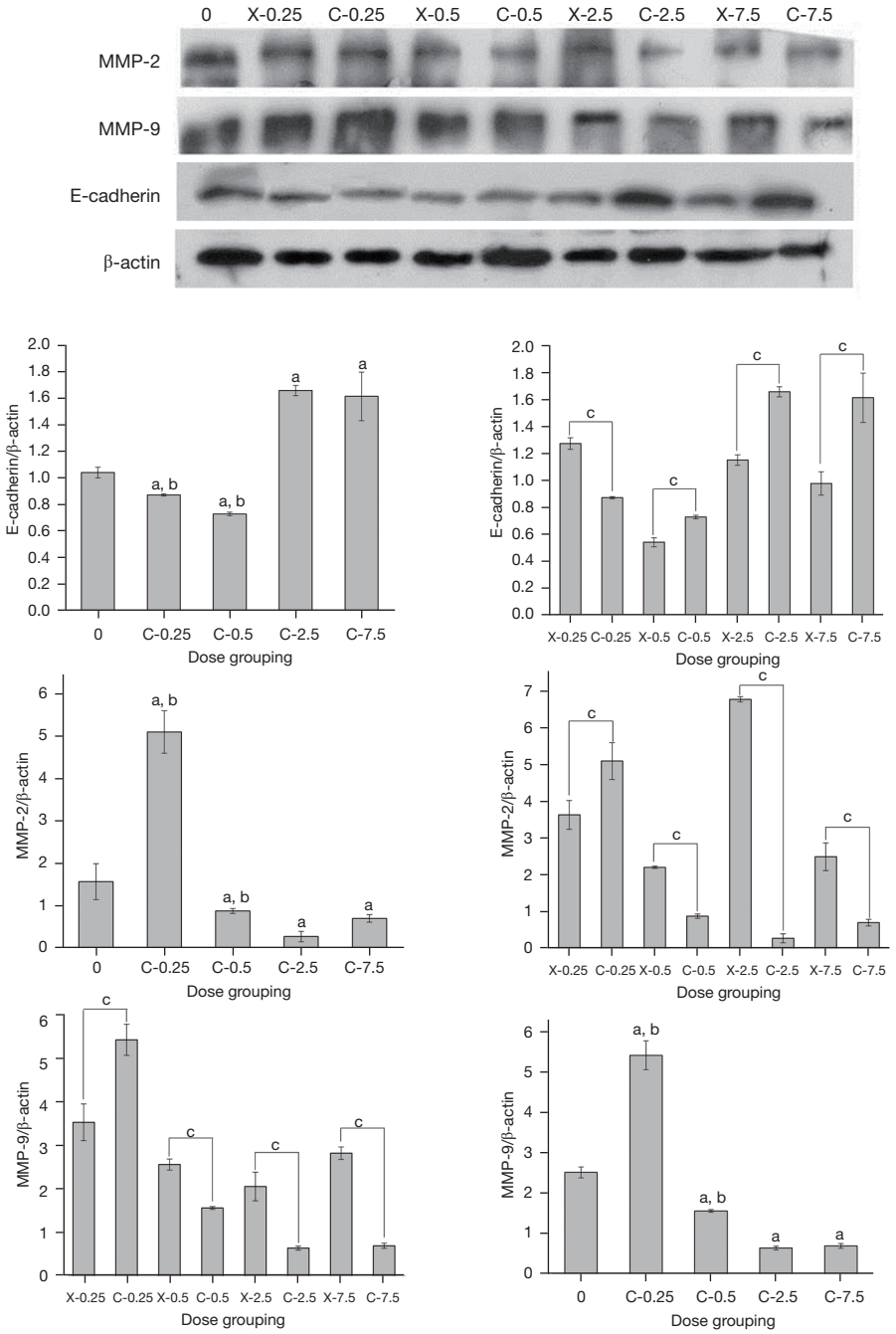

Figure 6 Effects of $^{12}C^{6+}$ and X-ray irradiation on the EMT-related proteins of B16F10 cells and statistical data. The protein bands represent the protein expression levels of MMP-2, MMP-9 and E-cadherin after different doses of $^{12}C^{6+}$ and X-ray irradiation. The histogram shows the relative protein expression level and statistical analysis obtained by systematically analyzing the gray value of the protein bands through Image-Pro Plus software. [a], the comparison between $^{12}C^{6+}$ irradiation group and blank control group, $P<0.05$; [b], the intra-group comparison of $^{12}C^{6+}$ irradiation group, $P<0.05$; [c], the comparison between the same dose of $^{12}C^{6+}$ and X-rays, $P<0.05$. C-0.25, C-0.5, C-2.5, C-7.5 represent $^{12}C^{6+}$ irradiation group at 0.25, 0.5, 2.5 and 7.5 Gy, respectively; X-0.25, X-0.5, X-2.5, X-7.5 represent X-ray irradiation group at 0.25, 0.5, 2.5 and 7.5 Gy, respectively. MMP, matrix metallopeptidase.

irradiation, the expressions of MMP-2 and MMP-9 were significantly increased (P<0.05). Moreover, the expression of E-cadherin was significantly increased after 2.5 GyE of $^{12}C^{6+}$ irradiation. The results revealed that compared with X-ray, $^{12}C^{6+}$ could inhibit MMP from cleaving the extracellular matrix by reducing the expressions of MMP-2 and MMP-9 in the B16F10 cells, thus inhibiting cell invasion and metastasis. In addition, $^{12}C^{6+}$ irradiation can also induce the expression of E-cadherin to inhibit EMT of cells. Previous clinical research from the Japan Institute of Radiological Sciences and other institutions revealed that after heavy ion radiotherapy, the local control rate of malignant melanoma patients was greatly improved, and the recurrence rate and distal metastasis rate decreased (25,28-31). The reason for this is that after heavy ion irradiation, the expression of metalloproteinase is inhibited, and malignant melanoma cells undergo EMT. These results provide a theoretical reference basis for further in-depth study of conventional and heavy ion radiotherapy for radiation-insensitive tumors.

In this study, the mechanism of the different therapeutic effects of $^{12}C^{6+}$ and X-ray radiotherapy on malignant melanoma was investigated, and preliminary research results were obtained. However, there were several limitations in the research process: the heavy ion irradiation platform was provided by the Heavy Ion Accelerator of the IMP, Chinese Academy of Sciences; at present, we have only two irradiation opportunities per year, and the irradiation time is limited. It is expected that multiple repeated experiments will be able to be performed after the conditions of heavy ion irradiation are improved. In addition, after irradiation with heavy ion $^{12}C^{6+}$, proliferation and invasion were inhibited and apoptosis of the B16F10 cells was induced, but the related signaling pathway and mechanism remain unclear. Therefore, the mechanism of signal pathway regulation must be further studied to explore the mechanism of heavy ion sensitivity in the treatment of radioresistant tumors to provide a theoretical basis and new ideas for the clinical treatment of other types of tumors with strong invasiveness and mobility and poor prognosis.

Conclusions

Based on the facts that malignant melanoma is not sensitive to conventional radiotherapy and that patients have a high mortality rate, this study investigated the effects of $^{12}C^{6+}$ and X-ray irradiation on the proliferation, apoptosis, cell cycle, invasion, migration, and EMT of B16F10 cells. Compared with X-ray, the $^{12}C^{6+}$ irradiation could significantly inhibit the proliferation of the B16F10 cells as well as reduce the expressions of anti-apoptotic proteins, induce the expressions of apoptotic proteins, and promote apoptosis. Moreover, $^{12}C^{6+}$ exhibited strong cancer-killing effects on malignant mouse melanoma B16F10 cells, and the $^{12}C^{6+}$ irradiation induced cell cycle regulation, resulting in G2/M arrest of the cells. The results further revealed that the B16F10 cells were highly radiosensitive to $^{12}C^{6+}$. Compared with X-ray, B16F10 cells irradiated by $^{12}C^{6+}$ significantly reduced the expressions of MMPs to inhibit extracellular matrix cleavage and, thus, inhibit cell invasion and metastasis. However, although the issue of the different therapeutic effects of heavy ion and X-ray radiotherapy on malignant melanoma was investigated and preliminary research results were obtained, several problems must be further studied. Also, animal model experiments will need to be conducted for further invasion and migration studies after ethics committee approval.

Acknowledgments

We are particularly grateful to all the people who have given us help on our article.

Funding: This study was supported by The Ministry of Science and Technology National Key R&D Project (No. SQ2018YFE020524); Lanzhou Heavy Ion Accelerated HIRFL User Cultivation Project (No. HIR19PY008).

Footnote

Reporting Checklist: The authors have completed the MDAR reporting checklist. Available at https://tcr.amegroups.com/article/view/10.21037/tcr-21-1692/rc

Data Sharing Statement: Available at https://tcr.amegroups.com/article/view/10.21037/tcr-21-1692/dss

Conflicts of Interest: All authors have completed the ICMJE uniform disclosure form (available at https://tcr.amegroups.com/article/view/10.21037/tcr-21-1692/coif). The authors have no conflicts of interest to declare.

Ethical Statement: The authors are accountable for all aspects of the work in ensuring that questions related to the accuracy or integrity of any part of the work are appropriately investigated and resolved. The study was conducted in accordance with the Declaration of Helsinki (as revised in 2013). The study was approved by ethics board

of the 940th Hospital of Joint Logistics Support Force of Chinese People's Liberation Army (No. 2021KYLL233) and individual consent for this retrospective analysis was waived.

References

1. Qin J, Li S, Zhang C, et al. Apoptosis and injuries of heavy ion beam and x-ray radiation on malignant melanoma cell. Exp Biol Med (Maywood) 2017;242:953-60.
2. Yang Z, Xie L, Huang Y, et al. Clinical features of malignant melanoma of the finger and therapeutic efficacies of different treatments. Oncol Lett 2011;2:811-15.
3. Kwiatkowska D, Kluska P, Reich A. Beyond PD-1 Immunotherapy in Malignant Melanoma. Dermatol Ther (Heidelb) 2019;9:243-57.
4. Mulder NH, van der Graaf WT, Willemse PH, et al. Dacarbazine (DTIC)-based chemotherapy or chemoimmunotherapy of patients with disseminated malignant melanoma. Br J Cancer 1994;70:681-3.
5. Robert C, Long GV, Brady B, et al. Nivolumab in previously untreated melanoma without BRAF mutation. N Engl J Med 2015;372:320-30.
6. Kumagai K, Nimura Y, Mizota A, et al. Arpc1b gene is a candidate prediction marker for choroidal malignant melanomas sensitive to radiotherapy. Invest Ophthalmol Vis Sci 2006;47:2300-4.
7. Koto M, Demizu Y, Saitoh JI, et al. Definitive Carbon-Ion Radiation Therapy for Locally Advanced Sinonasal Malignant Tumors: Subgroup Analysis of a Multicenter Study by the Japan Carbon-Ion Radiation Oncology Study Group (J-CROS). Int J Radiat Oncol Biol Phys 2018;102:353-61.
8. Hasebe M, Yoshikawa K, Nishii R, et al. Usefulness of 11C-methionine-PET for predicting the efficacy of carbon ion radiation therapy for head and neck mucosal malignant melanoma. Int J Oral Maxillofac Surg 2017;46:1220-8.
9. Prinzen T, Klein M, Hallermann C, et al. Primary head and neck mucosal melanoma: Predictors of survival and a case series on sentinel node biopsy. J Craniomaxillofac Surg 2019;47:1370-7.
10. Brenner DJ, Ward JF. Constraints on energy deposition and target size of multiply damaged sites associated with DNA double-strand breaks. Int J Radiat Biol 1992;61:737-48.
11. Wu G, Lin C, Yang D. Novel loop interactions within a parallel-stranded G-quadruplex formed in the human BCL-2 proximal promoter. Cancer Res 2017;77:abstr 5225.
12. van Hamburg JP, de Bruijn MJ, Dingjan GM, et al. Cooperation of Gata3, c-Myc and Notch in malignant transformation of double positive thymocytes. Mol Immunol 2008;45:3085-95.
13. Carruthers R, Ahmed SU, Strathdee K, et al. Abrogation of radioresistance in glioblastoma stem-like cells by inhibition of ATM kinase. Mol Oncol 2015;9:192-203.
14. Fernandez-Capetillo O, Lee A, Nussenzweig M, et al. H2AX: the histone guardian of the genome. DNA Repair (Amst) 2004;3:959-67.
15. Shrivastav M, Miller CA, De Haro LP, et al. DNA-PKcs and ATM co-regulate DNA double-strand break repair. DNA Repair (Amst) 2009;8:920-9.
16. Leadon SA, Dunn AB, Ross CE. A novel DNA repair response is induced in human cells exposed to ionizing radiation at the G1/S-phase border. Radiat Res 1996;146:123-30.
17. Farahmand AM, Ehsani AH, Mirzaei M, et al. Patients' Characteristics, Histopathological Findings, and Tumor Stage in Different Types of Malignant Melanoma: A Retrospective Multicenter Study. Acta Med Iran 2017;55:316-23.
18. Kalluri R, Weinberg RA. The basics of epithelial-mesenchymal transition. J Clin Invest 2009;119:1420-8. Erratum in: J Clin Invest. 2010 May 3;120(5):1786.
19. Wells A, Chao YL, Grahovac J, et al. Epithelial and mesenchymal phenotypic switchings modulate cell motility in metastasis. Front Biosci (Landmark Ed) 2011;16:815-37.
20. Shin J, Song IS, Pak JH, et al. Upregulation of annexin A1 expression by butyrate in human melanoma cells induces invasion by inhibiting E-cadherin expression. Tumour Biol 2016;37:14577-84.
21. Yan YR, Xie Q, Li F, et al. Epithelial-to-mesenchymal transition is involved in BCNU resistance in human glioma cells. Neuropathology 2014;34:128-34.
22. Muschel RJ, Yong J. The Gelatinases, MMP-2 and MMP-9-Implications for Invasion and Metastasis. In: Foidart

JM, Muschel RJ. editors. Proteases and Their Inhibitors in Cancer Metastasis. Cancer Metastasis — Biology and Treatment, vol 4. Dordrecht: Springer, 2002.
23. Sienel W, Polzer B, Elshawi K, et al. Cellular localization of EMMPRIN predicts prognosis of patients with operable lung adenocarcinoma independent from MMP-2 and MMP-9. Mod Pathol 2008;21:1130-8.
24. Yan J, Liu Y, Zhao Q, et al. The influencing factors and calculation method of RBE in heavy ion treatment of tumors. Journal of Radiation Research and Radiation Processing 2015;33:8.
25. Wambersie A, Menzel HG, Andreo P, et al. Isoeffective dose: a concept for biological weighting of absorbed dose in proton and heavier-ion therapies. Radiat Prot Dosimetry 2011;143:481-6.
26. Aninditha KP, Weber KJ, Brons S, et al. In vitro sensitivity of malignant melanoma cells lines to photon and heavy ion radiation. Clin Transl Radiat Oncol 2019;17:51-6.
27. Saito K, Funayama T, Yokota Y. Histone Deacetylase Inhibitors Sensitize Murine B16F10 Melanoma Cells to Carbon Ion Irradiation by Inducing G1 Phase Arrest. Biol Pharm Bull 2017;40:844-51.
28. Vitolo V, Fossati P, Bonora M, et al. EP-1350: Malignant mucosal melanoma in the upper aerodigestive tract treated with carbon ion RT at CNAO: preliminary results. Radiother Oncol 2015;115:S728.
29. Naganawa K, Koto M, Takagi R, et al. Long-term outcomes after carbon-ion radiotherapy for oral mucosal malignant melanoma. J Radiat Res 2017;58:517-22
30. Koto M, Demizu Y, Saitoh JI, et al. Multicenter Study of Carbon-Ion Radiation Therapy for Mucosal Melanoma of the Head and Neck: Subanalysis of the Japan Carbon-Ion Radiation Oncology Study Group (J-CROS) Study (1402 HN). Int J Radiat Oncol Biol Phys 2017;97:1054-60.
31. Hayashi K, Koto M, Ikawa H, et al. Efficacy and safety of carbon-ion radiotherapy for lacrimal gland carcinomas with extraorbital extension: a retrospective cohort study. Oncotarget 2018;9:12932-40.

Cite this article as: Zhang LP, Li S, Zhang H, Li Q, Liu Y, Li FF, Gong DJ. Effects of heavy ions ($^{12}C^{6+}$) on malignant melanoma B16F10 cells. Transl Cancer Res 2022;11(6):1616-1629. doi: 10.21037/tcr-21-1692

Supplementary

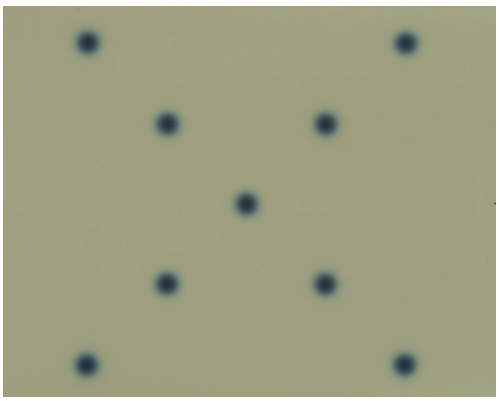

Figure S1 The typical image of independent dose verification in the place of the specimen using film during carbon ion irradiation.

https://dx.doi.org/10.21037/tcr-21-1692